Assessment of Rock Stiffness and Deformability from Dynamic Elastic Properties: A Log-Based Workflow for the Niger Delta Basin

Priscilla E. Ikioda[1], Etim D. Uko[2], Charles O. Ofeogbu[3], Olatunji S. Ayanninuola[4], Onengiyeofori A. Davies[5]

[1,2,3,4]Physics Department, Nasarawa State University, Keffi, Nasarawa State, Nigeria.

[5]Physics Department, Rivers State University, Port Harcourt, Rivers State, Nigeria.

DOI: https://doi.org/10.51584/IJRIAS.2025.100800102

Received: 10 August 2025; Accepted: 19 August 2025; Published: 18 September 2025

ABSTRACT

This study evaluates rock stiffness and deformability in the Niger Delta Basin using a log-based geomechanical workflow applied to the WABI Field. Gamma ray and resistivity log correlation identified reservoir intervals in six wells, with sonic data available for two (AKOS-009, AKOS-002). Dynamic elastic parameters—P-wave velocity, S-wave velocity, Young's modulus, bulk modulus, shear modulus, Poisson's ratio, and unconfined compressive strength—were derived from sonic and density logs to characterize mechanical properties. Results show consistent depth-dependent increases in velocities and elastic moduli, reflecting compaction-driven lithification, porosity reduction, and enhanced mechanical competence. Poisson's ratio decreases with depth, indicating a shift toward more brittle behavior. AKOS-002 displays broader property ranges and greater scatter than AKOS-009, suggesting higher lithological heterogeneity, variable cementation, and differences in consolidation. These variations highlight both regional compaction trends and lateral variability in rock mechanical behavior, with implications for seismic-to-well calibration, fracture prediction, wellbore stability, and reservoir geomechanical modeling.

Index Terms: Stiffness, Deformability, Reservoir, Elastic Parameters, Niger Delta

INTRODUCTION

The mechanical behaviour of reservoir rocks is a key factor in hydrocarbon exploration and production. It influences wellbore stability, sand production, compaction, and the performance of stimulation techniques such as hydraulic fracturing [1]. Two fundamental descriptors of this behaviour are rock stiffness, which is the resistance of the rock to deformation under stress [2], and rock deformability, which is the ability of the rock to change shape or volume when subjected to applied loads [3]. These properties are expressed through elastic parameters such as Young's modulus, shear modulus, bulk modulus, and Poisson's ratio, which are essential inputs for geomechanical modelling.

Elastic parameters can be determined through laboratory testing of core samples, known as static measurements, or derived from well log data, known as dynamic measurements. Although static measurements are often preferred for detailed geomechanical modelling, they are not always available due to the cost and limited coverage of core acquisition [4]. This limitation is common in the Niger Delta Basin, where many wells lack continuous core data. In such situations, dynamic elastic parameters derived from well logs provide a practical alternative for reservoir characterisation and preliminary geomechanical evaluation.

Dynamic elastic properties are commonly estimated from conventional wireline logs such as compressional sonic velocity (V_p) and bulk density (ρ_b) using established rock physics relationships. While the absolute values of dynamic parameters differ from those obtained in the laboratory, they reliably reflect relative variations in mechanical properties [5]. These variations can be used to identify stratigraphic and lithological changes as well as zones with contrasting mechanical behaviour, which is critical for reservoir stability assessment.

The Niger Delta Basin is a prolific hydrocarbon province characterised by thick successions of interbedded

ISSN No. 2454-6194 | DOI: 10.51584/IJRIAS |Volume X Issue VIII August 2025

sandstones and shales deposited in deltaic to shallow marine environments [6, 7]. The WABI Field, located in the central part of the basin (Figure 1), contains clastic reservoirs with significant heterogeneity in lithology and mechanical behaviour. Understanding these variations is important for optimising drilling programmes, reducing non-productive time, and managing production risks.

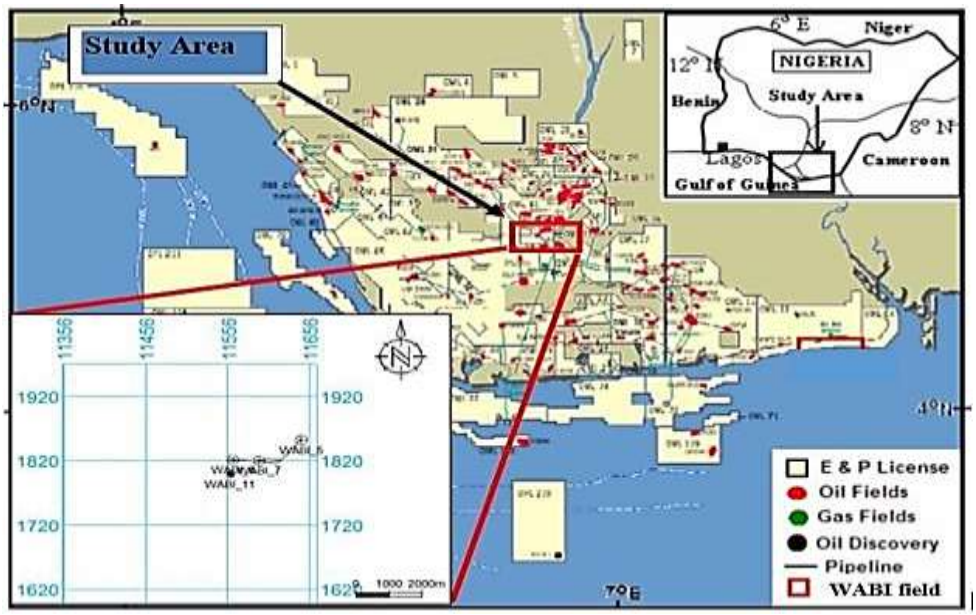

Fig. 1: Location map of study area

This study assesses the stiffness and deformability of reservoir rocks in the WABI Field by deriving dynamic elastic parameters from well logs using empirical models. Petrel software is used for data preparation, depth matching, lithology interpretation, and computation of elastic parameters. Microsoft Excel is employed for empirical modelling, cross-plotting, and statistical analysis. The workflow includes data quality control, computation of elastic moduli, zonation of mechanical properties, and interpretation in the context of reservoir stability.

METHODOLOGY

Data Acquisition

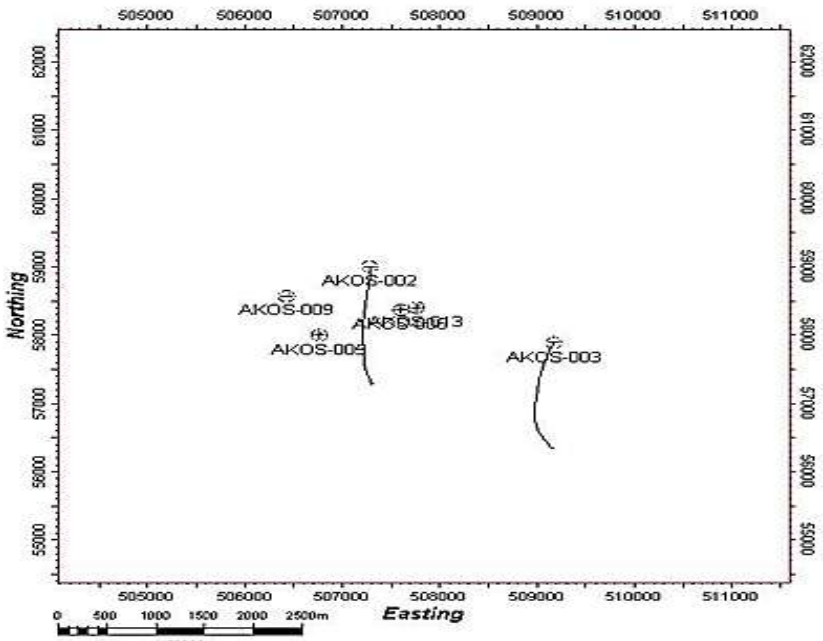

Fig. 2: Position of the well in the field

ISSN No. 2454-6194 | DOI: 10.51584/IJRIAS |Volume X Issue VIII August 2025

The available dataset consists of a suite of well logs, including Gamma Ray, Resistivity, Density, and Sonic logs. The spatial locations of these wells are presented in Figure 2. For reference purposes, the wells have been assigned general identifiers: AKOS-002, AKOS-003, AKOS-005, AKOS-006, AKOS-009, and AKOS-013.

Well Log Correlation

Well log correlation was carried out to identify and differentiate lithologies within the reservoir interval using gamma ray and resistivity logs. The gamma ray log was used to estimate shale content, with lower readings indicating cleaner sandstones and higher readings reflecting shalier zones. Resistivity logs were then compared against the gamma ray trends to refine lithology interpretation, as clean sandstones typically exhibit higher resistivity due to hydrocarbon saturation, while shales and water-bearing zones show lower resistivity. This correlation provided a reliable basis for defining reservoir and non-reservoir units prior to the computation of dynamic elastic parameters.

Velocity Computation

P-wave velocity was calculated from the transit time recorded on the sonic log using the empirical relationship provided by Asquith et al. (2004), as presented in equation 1.

$$V_p = \Delta t_P^{-1} \qquad \mathbf{1}$$

To maintain consistency, the compressional wave velocity (V_p) obtained from sonic transit time was multiplied by 1,000,000 to convert from the unit derived from transit time in $\mu s/ft$ to ft/s. This value was then divided by 3.2808 to convert from ft/s to m/s, based on the relationship $1\ m/s\ =\ 3.2808\ ft/s$.

Reservoirs in the Niger Delta are typically classified as shaley sandstones [8]. Consequently, the shear wave velocity (Vs) in m/s for the reservoir interval was estimated using the clay-adjusted form of the standard inverse Castagna equation for shaley sandstones, as presented by Davies et. al. [9] and shown in equation 2.

$$V_s = 0.804V_p - 1032 \qquad \mathbf{2}$$

Elastic Parameter Estimation

The theory of elasticity describes the relationship between applied forces and the resulting deformation of a rock, assuming the material is elastic, isotropic, and homogeneous. Under these conditions, stress and strain are linearly related, and the deformation is fully recoverable once the force is removed. The proportionality constant in this relationship is Young's modulus, which reflects the stiffness of the material [10]. In this study, the dynamic Young's modulus (E_{dyn}) of the reservoir was calculated using empirical relationships that incorporate compressional wave velocity (V_p), shear wave velocity (V_s), and bulk density (ρ) derived from the density log, as presented in equation 3.

$$E_{dyn} = \frac{\rho V_S^2(3V_P^2 - 4V_S^2)}{(V_P^2 - V_S^2)} \qquad \mathbf{3}$$

The bulk modulus represents a reservoir rock's resistance to uniform compression, which directly relates to its stiffness and its capacity to deform under stress. In geomechanics and reservoir engineering, this property is essential for evaluating how rocks respond to changes in pore pressure and confining stress, both of which influence stability and production performance [11]. In this study, the dynamic bulk modulus (k_{dyn}) was estimated to quantify the stiffness and deformability of the reservoir units. The calculation was based on the empirical relationship between elastic wave velocities and bulk density proposed by Mavko et al. [12], as expressed in equation 4.

$$K_{dyn} = \rho\left(V_P^2 - \frac{4}{3}V_S^2\right) \qquad \mathbf{4}$$

ISSN No. 2454-6194 | DOI: 10.51584/IJRIAS |Volume X Issue VIII August 2025

The dynamic shear modulus, or modulus of rigidity, reflects the ability of a reservoir rock to resist shear deformation and is directly related to its stiffness and deformability. It influences how the rock responds to shear stress, which affects its seismic response, mechanical stability during drilling, and behaviour under enhanced recovery operations [13]. In this study, the dynamic shear modulus (G_{dyn}) of the reservoir interval was calculated using the empirical relationship proposed by Mavko et al. [12], incorporating density values and shear wave velocity to quantify the rock's mechanical behaviour for geomechanical assessment, as seen in equation 5.

$$G_{dyn} = \rho V_S^2 \qquad \textbf{5}$$

Poisson's ratio is a key elastic parameter that links rock stiffness to its ability to deform laterally when subjected to axial stress. It reflects the balance between rigidity and deformability, influencing how stresses are distributed within the reservoir and affecting fracture initiation, propagation, and seismic wave response. Accurate estimation of Poisson's ratio is therefore important for evaluating mechanical stability and optimising drilling, stimulation, and reservoir management strategies. In this study, dynamic Poisson's ratio (υ_{dyn}) was calculated from elastic wave velocities using the relationship described by Archer and Rasouli [14], as presented in the corresponding equation.

$$\nu_{dyn} = \frac{V_P^2 - 2V_S^2}{2(V_P^2 - V_S^2)} \qquad \textbf{6}$$

Unconfined compressive strength (UCS) represents the maximum axial load a rock can withstand without lateral confinement and is a key indicator of rock stiffness and deformability. Accurate UCS estimation supports wellbore stability analysis, hydraulic fracturing design, sand production prediction, and overall reservoir management [15]. In this study, UCS (in MPa) was derived from dynamic Young's modulus (in GPa) using an empirical model developed for shaley sandstones by Chang et. al. [16], as shown in equation 7, providing a link between log-derived elastic properties and the mechanical strength of the reservoir rock.

$$UCS = 0.6E_{dyn} - 2 \qquad \textbf{7}$$

Data Analysis

The estimated parameters will then be plotted against depth in their respective wells, showing vertical variation of the computed parameters

RESULTS AND DISCUSSION

Results

The results obtained from the analysis are shown below.

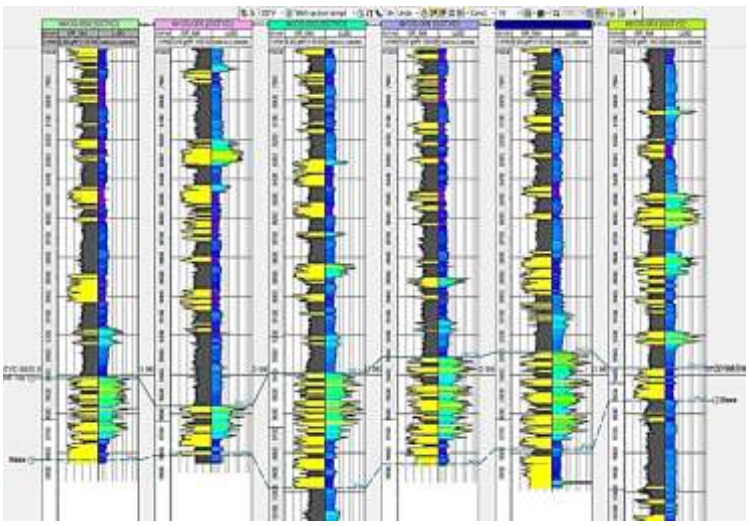

Fig. 3: Delineated reservoirs from well logs

ISSN No. 2454-6194 | DOI: 10.51584/IJRIAS |Volume X Issue VIII August 2025

Table 1: Average Values of estimated relative permeability for both reservoirs from the five well logs

WELL NAME	RESERVOIR DEPTH RANGE (ft)
AKOS-009	9406-9854
AKOS-005	9560-9820
AKOS002	9385-9980
AKOS-006	9310-9860
AKOS-013	9290-9970
AKOS-003	9370-9530

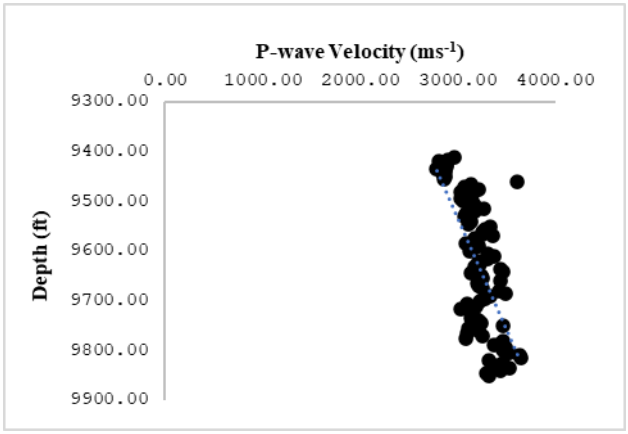

Fig. 4: P-wave velocities plotted against depth in AKOS-009

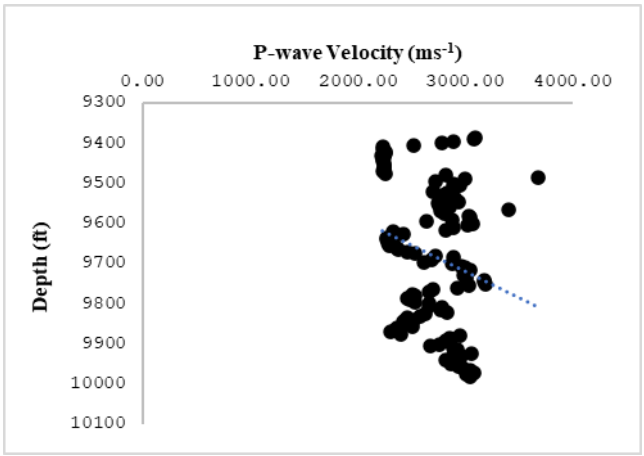

Fig. 5: P-wave velocities plotted against depth in AKOS-002

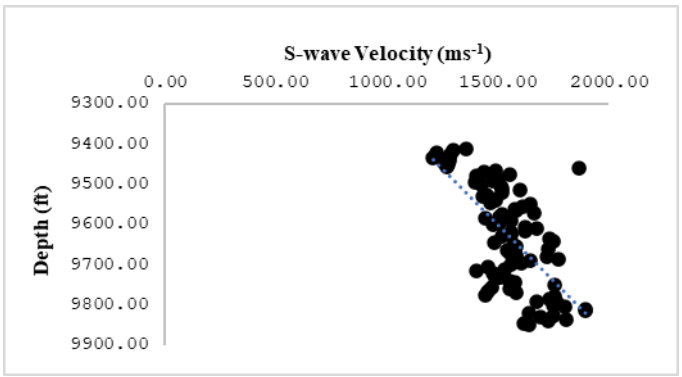

Fig. 6: S-wave velocities plotted against depth in AKOS-009

ISSN No. 2454-6194 | DOI: 10.51584/IJRIAS |Volume X Issue VIII August 2025

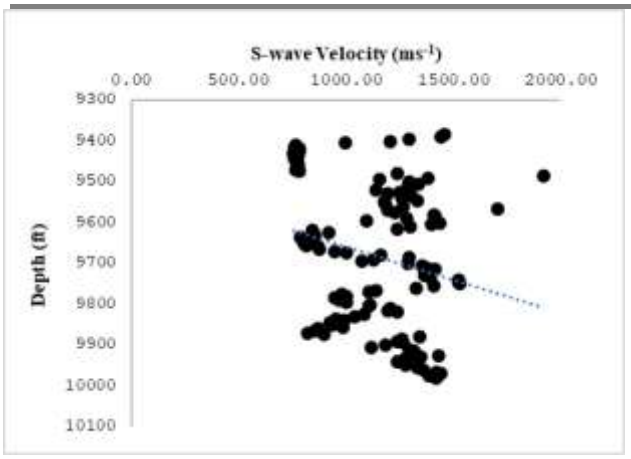

Fig. 7: S-wave velocities plotted against depth in AKOS-002

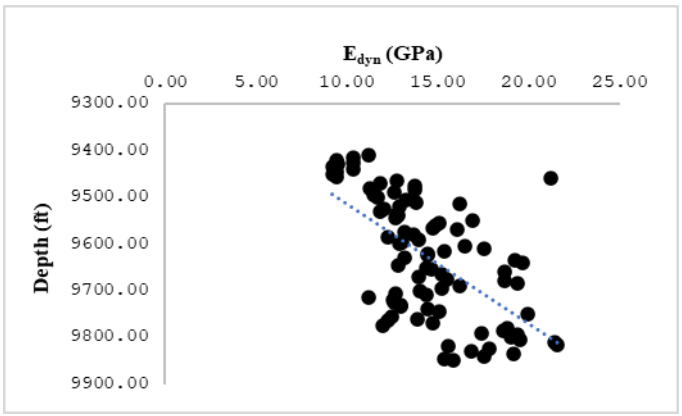

Fig. 8: Dynamic Young's Modulus plotted against depth in AKOS-009

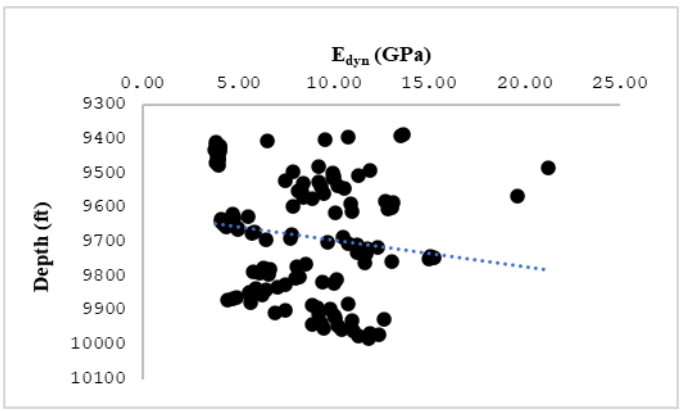

Fig. 9: Dynamic Young's Modulus plotted against depth in AKOS-002

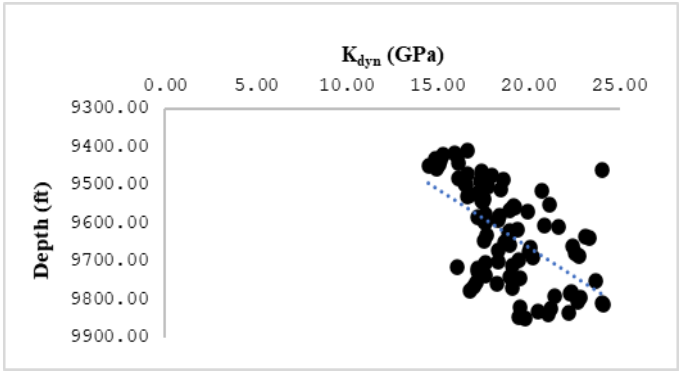

Fig. 10: Dynamic Bulk Modulus plotted against depth in AKOS-009

ISSN No. 2454-6194 | DOI: 10.51584/IJRIAS |Volume X Issue VIII August 2025

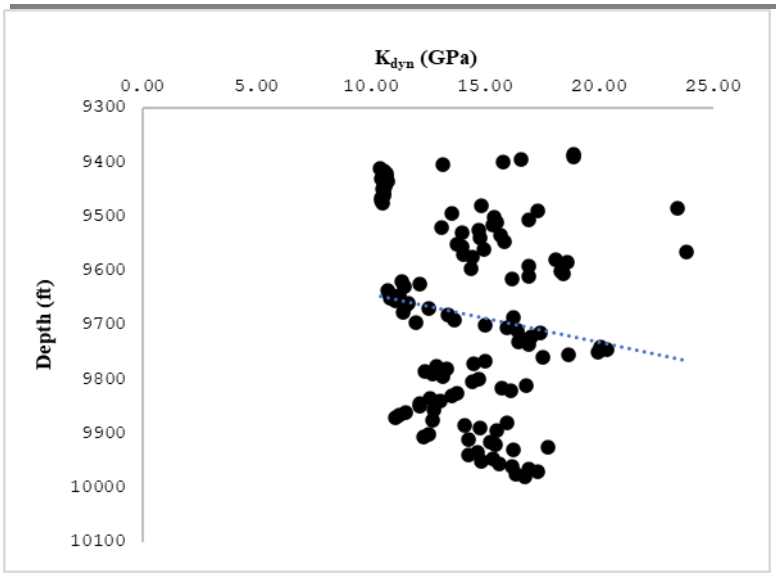

Fig. 11: Dynamic Bulk Modulus plotted against depth in AKOS-002

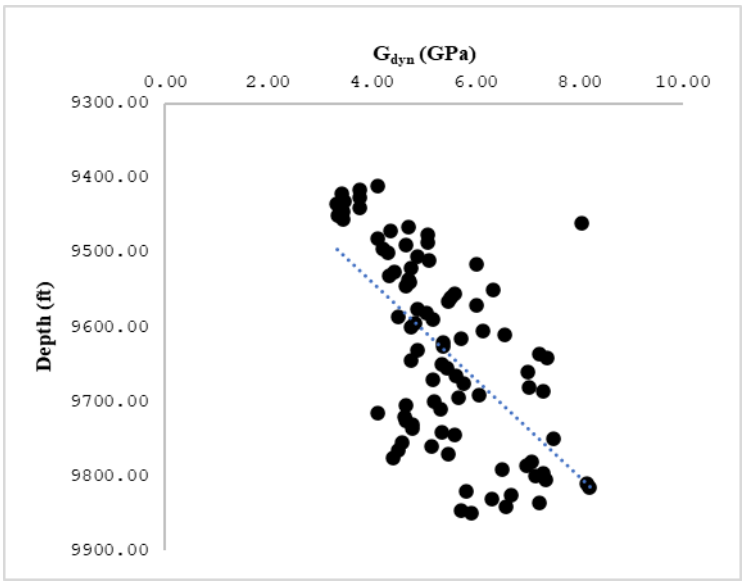

Fig. 12: Dynamic Shear Modulus plotted against depth in AKOS-009

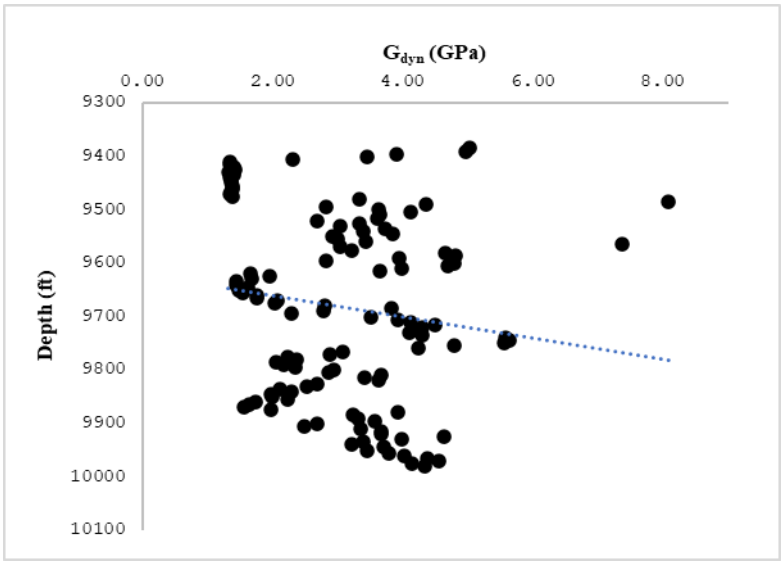

Fig. 13: Dynamic Shear Modulus plotted against depth in AKOS-002

ISSN No. 2454-6194 | DOI: 10.51584/IJRIAS |Volume X Issue VIII August 2025

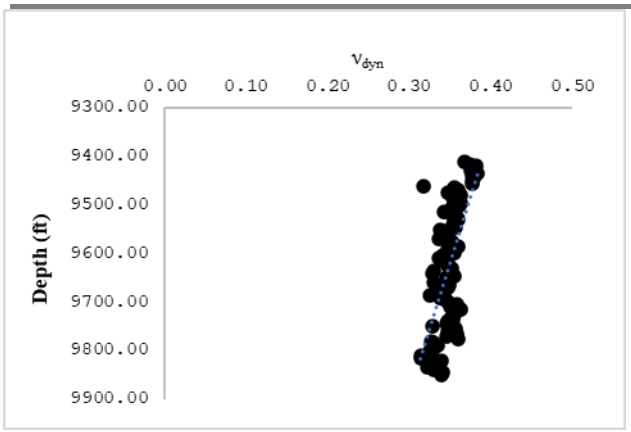

Fig. 14: Dynamic Poisson ratio plotted against depth in AKOS-009

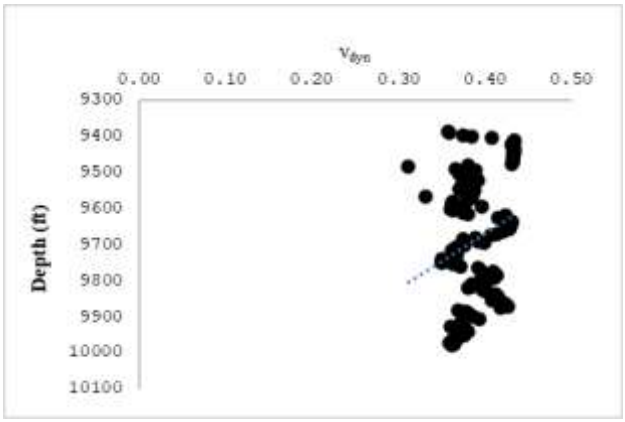

Fig. 15: Dynamic Poisson ratio plotted against depth in AKOS-002

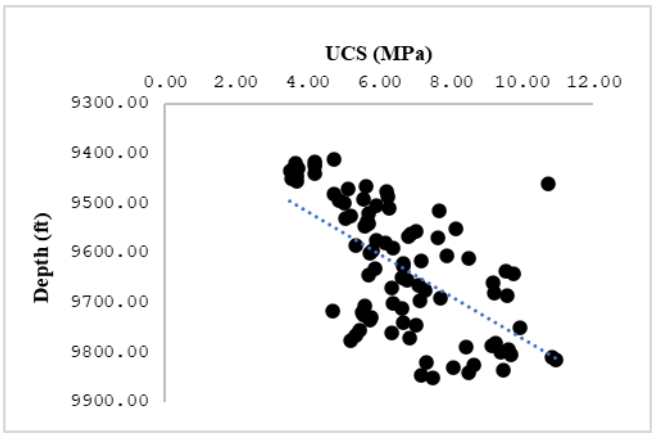

Fig. 16: Unconfined Compressive Stress plotted against depth in AKOS-009

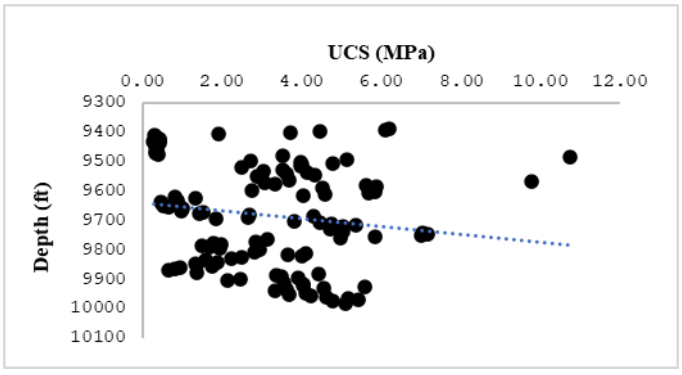

Fig. 17: Unconfined Compressive Stress plotted against depth in AKOS-002

ISSN No. 2454-6194 | DOI: 10.51584/IJRIAS |Volume X Issue VIII August 2025

DISCUSSION

The well log correlation done with the available well logs (figure 3) revealed a reservoir unit at depth intervals that are shown in table 1 in the study area.

Assessing the stiffness and deformability of the reservoir rock in the study area was done by carrying a geomechanical analysis of the WABI Field reservoir relative to sonic and density log data which was used to derive dynamic elastic parameters, which are direct indicators of rock stiffness and deformability. Since sonic log data were available only in two wells (AKOS-009 and AKOS-002) out of the six wells in the study area, the analysis and subsequent interpretation of stiffness and deformability variations were restricted to these wells

The depth versus p-wave velocity plots for wells AKOS-009 and AKOS-002 (figures 4 and 5) show a clear increase in P-wave velocity with depth, consistent with compaction-driven lithification and porosity reduction in sedimentary formations. In AKOS-009, velocities rise from about 2200 to 3300 ms^{-1} between approximately 9400 ft and 9900 ft, following a typical compaction trend according to Salah et. al. [17]. Scatter in the data is likely due to lithological variability, interbedded sand and shale units, fluid effects, or logging conditions [18]. In AKOS-002, velocities range from 2226.44 to 3674.95 ms^{-1} over depths of 9385 to 9980 ft, also showing a positive depth trend. The broader range and higher upper values in AKOS-002 suggest the presence of more competent lithologies or stronger cementation at greater depths. The scatter observed in both datasets reflects local heterogeneities in lithology, fluid saturation, or microstructure. Combined, these results, according to Fawad et. al. [19] support a regional model of depth-dependent mechanical strengthening and acoustic velocity enhancement, which is important for seismic-to-well ties, time–depth conversion, impedance modeling, and reservoir characterization.

Depth versus S-wave velocity plots for AKOS-009 and AKOS-002 (figures 6 and 7) show a clear increase in velocity with depth, reflecting progressive sediment compaction, lithification, and increased mechanical competence. In AKOS-009, velocities rise from about 800 to over 1700 ms^{-1} between approximately 9400 ft and 9900 ft, consistent with reduced porosity, enhanced grain contacts, and stiffer formations under greater overburden stress [17, 20]. Scatter in the data indicates lithological heterogeneities such as alternating sand–shale layers, fractures, or fluid variations. Since S-wave velocity is sensitive to shear rigidity and less affected by fluid type, according to Quintal et. al. [21], the trend confirms increasing consolidation with depth. In AKOS-002, velocities range from 758.06 to 1922.66 ms^{-1} between 9385 ft and 9980 ft, showing a similar positive depth trend with greater scatter and a broader range than AKOS-009. This suggests more variable lithology, mineral composition, clay content, or cementation [13, 22]. The comparison supports a regional compaction trend while indicating lateral variability in elastic properties, which is important for geomechanical modeling, fracture prediction, and seismic attribute analysis.

Depth versus dynamic Young's modulus plots for wells AKOS-009 and AKOS-002 (figures 8 and 9) show a general increase in stiffness with depth, reflecting compaction-driven porosity reduction, improved grain contact, and enhanced elastic properties. In AKOS-009, values range from about 6 GPa to over 20 GPa between 9400 ft and 9900 ft, matching corresponding increases in P-wave and S-wave velocities and indicating improved rock competence [23]. Scatter in the data reflects lithological variation, pore fluid differences, and microfractures [24]. In AKOS-002, dynamic Young's modulus ranges from 3.81 GPa to 21.21 GPa between 9385 ft and 9980 ft, also increasing with depth but showing more pronounced scatter. The broader range in AKOS-002 suggests greater lithological variability or differences in cementation and consolidation, with lower values likely from clay-rich or compliant layers and higher values from better-consolidated sandstones or carbonate-rich facies [25]. Together, these results confirm a regional trend of increasing stiffness with depth and point to lateral variations in mechanical properties, which are important for reservoir geomechanical modeling, elastic property mapping, and wellbore stability assessments.

The dynamic bulk modulus for well AKOS-009, between 9400 ft and 9900 ft, ranges from 14.47 to 24.10 GPa and shows a clear depth-related increase with some scatter (figure 10), reflecting progressive compaction and consolidation that enhance resistance to volumetric deformation under confining pressure [26]. This trend indicates decreasing compressibility with depth, consistent with porosity reduction and improved grain-to-grain contact from lithostatic loading, while scatter likely reflects lithological heterogeneity, variable fluid saturation,

or microstructural features such as fractures [27]. Well AKOS-002, between 9385 ft and 9980 ft, shows a similar upward trend (figure 11), ranging from 10.44 to 23.82 GPa, but with greater variability that suggests more pronounced lithological heterogeneity, possibly from interbedded sands, shales, or carbonates, and differences in cementation or fluid content [28]. These findings align with P-wave, S-wave, and dynamic Young's modulus trends, supporting a regional model of depth-dependent mechanical strengthening. The results are significant for seismic impedance modeling, fluid substitution analysis, and assessing reservoir integrity under production-induced stress changes.

In AKOS-009, the dynamic shear modulus between 9400 and 9900 ft ranges from 3.32 to 8.20 GPa, showing a general increase with depth despite noticeable scatter (figure 12). This trend indicates progressive enhancement in shear rigidity due to compaction and lithification under increasing overburden stress [29], consistent with S-wave velocity trends in the same interval. Scatter likely reflects heterogeneities such as interbedded lithologies, clay variability, microfractures, or changes in pore fluid composition, all influencing shear stiffness at localized scales [30]. In AKOS-002, values range from 1.33 to 8.08 GPa over depths of 9385 to 9980 ft, also increasing with depth (figure 13) but with a lower minimum modulus, suggesting more compliant or clay-rich intervals at shallower depths [31]. The greater scatter in AKOS-002 points to higher lithological and mechanical variability from factors like variable cementation, natural fractures, and fluid-filled pores. Since dynamic shear modulus relates directly to S-wave velocity and rock matrix stiffness, these results highlight depth-dependent mechanical strengthening across the field while revealing localized differences in rock fabric and composition, with implications for stress modeling, borehole stability, and seismic interpretation.

Dynamic Poisson's ratio for the reservoir interval in well AKOS-009 (9400–9900 ft) ranges from 0.31 to 0.38, showing a consistent decrease with depth and minimal scatter (figure 14), indicating increased rigidity and a shift toward more brittle behavior as compaction reduces porosity and lithology transitions to more consolidated formations [32, 33]. This trend aligns with increasing shear modulus and reduced fluid influence at greater depths, suggesting improved mechanical competence and higher fracturing potential [34]. In well AKOS-002 (9385–9980 ft), Poisson's ratio ranges from 0.31 to 0.43, also decreasing with depth but with greater scatter (figure 15), reflecting more pronounced lithological heterogeneity, variations in mineralogy, consolidation, pore pressure, or microfracturing. Higher shallow values (>0.40) in AKOS-002 indicate more compliant or fluid-rich units, while lower deep values mark a transition to stiffer, compacted rock. Comparison of both wells confirms a regional trend of decreasing Poisson's ratio with depth while highlighting local variability, providing insights into rock brittleness, fracture propagation potential, and depth-dependent geomechanical evolution relevant to reservoir characterization and wellbore design.

The unconfined compressive strength (UCS) for the reservoir interval in well AKOS-009 (9400–9900 ft) ranges from 3.51 to 10.93 MPa, showing a depth-dependent increase (figure 16) that reflects progressive strengthening and consolidation due to overburden stress and compaction [35]. This trend aligns with increases in dynamic elastic moduli and indicates a transition from weaker, less consolidated formations to more competent rock units. Scatter in the data likely results from variations in lithology, cementation, fractures, or grain alignment, which influence rock integrity. In well AKOS-002 (9385–9980 ft), UCS values range from 0.28 to 10.72 MPa, also increasing with depth but with greater scatter and a broader range, suggesting mechanically weaker zones at shallower depths, possibly due to less consolidated lithologies, higher clay content, or elevated pore pressure [1]. The differences between the wells highlight lateral variability in rock mechanical properties, driven by heterogeneity in mineral composition, cementation, and structural features. Collectively, these results provide a detailed geomechanical framework for strength classification, borehole stability modeling, fracture propagation assessment, and site-specific well planning.

CONCLUSIONS

The log-based assessment confirms a strong depth-dependent increase in stiffness and reduction in deformability across the reservoir interval, driven by compaction and lithification processes. P-wave and S-wave velocity trends, coupled with rising dynamic elastic moduli, indicate progressive strengthening of the rock framework with depth. The observed decrease in Poisson's ratio suggests increasing brittleness, enhancing the potential for fracture propagation in deeper, better-consolidated units. Lateral variations between AKOS-009 and AKOS-002 reflect differences in lithology, mineral composition, clay content, and cementation, which must be accounted

ISSN No. 2454-6194 | DOI: 10.51584/IJRIAS |Volume X Issue VIII August 2025

for in field-scale geomechanical models. These findings provide a quantitative basis for predicting rock mechanical behavior, improving seismic interpretation, optimizing drilling strategies, and managing reservoir integrity during production

REFERENCES

1. Lu, Y., C. Li, Z. He, M. Gao, R. Zhang, C. Li, and H. Xie, Variations in the physical and mechanical properties of rocks from different depths in the Songliao Basin under uniaxial compression conditions. Geomechanics and Geophysics for Geo-Energy and Geo-Resources, 2020. 6(3): p. 43.
2. Xu, Y. and M. Cai, Influence of loading system stiffness on post-peak stress–strain curve of stable rock failures. Rock Mechanics and Rock Engineering, 2017. 50(9): p. 2255-2275.
3. Brady, B. and E. Brown, Rock strength and deformability, in Rock Mechanics for underground mining: Third edition. 2007, Springer. p. 85-141.
4. Cheremisin, A., Y. Petrakov, A. Sobolev, S. Stishenko, O. Tatur, K. Chettykbaeva, and A. Ocheretyanyy. Geomechanical Modeling Under Industry Standards. in SPE Russian Petroleum Technology Conference. 2018. SPE.
5. Zhang, Q.B. and J. Zhao, A review of dynamic experimental techniques and mechanical behaviour of rock materials. Rock Mechanics and Rock Engineering, 2014. 47(4): p. 1411-1478.
6. Doust, H. and E. Omatsola, Niger delta. American Association of Petroleum Geologists Memoir, 1989. 48: p. 201-238.
7. Chukwu, G., The Niger Delta complex basin: Stratigraphy, structure and hydrocarbon potential. Journal of Petroleum Geology, 1991. 14: p. 211-220.
8. Makeen, Y.M., W.H. Abdullah, H.A. Ayinla, M.H. Hakimi, and S.-G. Sia, Sedimentology, diagenesis and reservoir quality of the upper Abu Gabra Formation sandstones in the Fula Sub-basin, Muglad Basin, Sudan. Marine Petroleum Geology, 2016. 77: p. 1227-1242.
9. Davies, D.H., O.A. Davies, and O.I. Horsfall, Determination of Geomechanical Properties of a typical Niger Delta Reservoir Rock Using Geophysical Well Logs. Asian Journal of Applied science Technology, 2019. 3(1): p. 222-233.
10. Sohail, G.M., Q. Yasin, A.E. Radwan, and M.Z. Emad, Estimating hardness and Young's modulus of shale using drill cuttings: Implications for hydraulic fracturing in shale gas reservoir development. Gas Science and Engineering, 2023. 118: p. 205116.
11. Zoback, M.D., Reservoir geomechanics. 2010: Cambridge university press.
12. Mavko, G., T. Mukerji, and J. Dvorkin, The rock physics handbook: Tools for seismic analysis of porous media. 2009: Cambridge university press.
13. Eshkalak, M.O., S.D. Mohaghegh, and S. Esmaili, Geomechanical properties of unconventional shale reservoirs. Journal of Petroleum Engineering, 2014. 2014(1): p. 961641.
14. Archer, S. and V. Rasouli, A log based analysis to estimate mechanical properties and in-situ stresses in a shale gas well in North Perth Basin. Journal of Transactions on Engineering Sciences, 2012. 81: p. 163-174.
15. Ahmadi, M., Advancing Geotechnical Evaluation of Wellbores: A Robust and Precise Model for Predicting Uniaxial Compressive Strength (UCS) of Rocks in Oil and Gas Wells. Applied Sciences, 2024. 14(22): p. 10441.
16. Chang, C., M.D. Zoback, and A. Khaksar, Empirical relations between rock strength and physical properties in sedimentary rocks. Journal of Petroleum Science and Engineering, 2006. 51(3-4): p. 223-237.
17. Salah, M.K., M. Alqudah, A.K. Abd El-Aal, and C. Barnes, Effects of porosity and composition on seismic wave velocities and elastic moduli of lower cretaceous rocks, central Lebanon. 2018. 66(5): p. 867-894.
18. Ghosh, S., A review of basic well log interpretation techniques in highly deviated wells. Journal of Petroleum Exploration and Production Technology, 2022. 12(7): p. 1889-1906.
19. Fawad, M., N.H. Mondol, J. Jahren, and K. Bjørlykke, Mechanical compaction and ultrasonic velocity of sands with different texture and mineralogical composition. Geophysical Prospecting, 2011. 59(4): p. 697-720.
20. Holt, R.M., O.-M. Nes, and E. Fjaer, In-situ stress dependence of wave velocities in reservoir and

overburden rocks. The Leading Edge, 2005. 24(12): p. 1268-1274.
21. Quintal, B., H. Steeb, M. Frehner, S.M. Schmalholz, and E.H. Saenger, Pore fluid effects on S-wave attenuation caused by wave-induced fluid flow. Geophysics, 2012. 77(3): p. L13-L23.
22. Leila, M., S. Sen, M. Abioui, and A. Moscariello, Investigation of pore pressure, in-situ stress state and borehole stability in the West and South Al-Khilala hydrocarbon fields, Nile Delta, Egypt. Geomechanics and Geophysics for Geo-Energy and Geo-Resources, 2021. 7(3): p. 1-16.
23. Kandil, M.E., A. Ali, M.R. Khodja, and T.I. Sølling, Exploring deep carbonate reservoir samples: Anisotropy and correlation of static and dynamic Young's moduli. Geophysics, 2022. 87(3): p. MR151-MR159.
24. Liu, J., P. Chen, K. Xu, H. Yang, H. Liu, and Y. Liu, Fracture stratigraphy and mechanical stratigraphy in sandstone: A multiscale quantitative analysis. Marine and Petroleum Geology, 2022. 145: p. 105891.
25. Sone, H. and M.D. Zoback, Mechanical properties of shale-gas reservoir rocks—Part 2: Ductile creep, brittle strength, and their relation to the elastic modulus. Geophysics, 2013. 78(5): p. D393-D402.
26. Lyu, C., J. Park, and J. Carlos Santamarina, Depth-dependent seabed properties: Geoacoustic assessment. Journal of Geotechnical and Geoenvironmental Engineering, 2021. 147(1): p. 04020151.
27. Avseth, P., T. Mukerji, G. Mavko, and J. Dvorkin, Rock-physics diagnostics of depositional texture, diagenetic alterations, and reservoir heterogeneity in high-porosity siliciclastic sediments and rocks—A review of selected models and suggested work flows. Geophysics, 2010. 75(5): p. 75A31-75A47.
28. Sharifi, J., M.R. Saberi, A. Javaherian, and N. Hafezi Moghaddas, Investigation of static and dynamic bulk moduli in a carbonate field. Exploration Geophysics, 2021. 52(1): p. 16-41.
29. Dusseault, M.B., Geomechanical challenges in petroleum reservoir exploitation. KSCE Journal of Civil Engineering, 2011. 15(4): p. 669-678.
30. Sharma, R., M. Prasad, M. Batzle, and S. Vega, Sensitivity of flow and elastic properties to fabric heterogeneity in carbonates. Geophysical Prospecting, 2013. 61(2): p. 270-286.
31. Li, D., J. Wei, B. Di, D. Shuai, L. Tian, and P. Ding, Effect of fluid saturation on the shear modulus of artificial clay-rich tight sandstones. Geophysical Journal International, 2020. 222(1): p. 15-26.
32. Zhang, J., H. Liu, S. Tong, L. Xing, X. Chen, and C. Su, Estimation of elastic parameters using two-term fatti elastic impedance inversion. Journal of Earth Science, 2015. 26(4): p. 556-566.
33. Dehghani, H., R. Penta, and J. Merodio, The role of porosity and solid matrix compressibility on the mechanical behavior of poroelastic tissues. Materials Research Express, 2018. 6(3): p. 035404.
34. Hou, Z., M. Gutierrez, A. Wang, A. Almrabat, and C. Yang, Mechanical properties and brittleness of shale with different degrees of fracturing-fluid saturation. Current Science, 2018. 115(6): p. 1163-1173.
35. Wang, J., Z. Jinliang, and J. Xie, Analysis of the factors that influence diagenesis in the terminal fan reservoir of fuyu oil layer in the southern Songliao basin, northeast China. Open Geosciences, 2018. 10(1): p. 866-881.